Automation of the Pneumatic Caisson Method
- Optimization of Excavation Using the Greedy Algorithm -

Hiroki Harada[1], Kiichiro Ishikawa[1], Taichi Terui[2], Yusen Inagawa[2], Kiyoshi Nakamura[2], Shinichi Tachibana[3], Shingo Tsugawa[3], Kotaro Nagahama[4] and Koji Terada[4]

[1] Department of Mechanical Engineering, Nippon Institute of Technology, Saitama, Japan
[2] OBAYASHI CORPORATION, Tokyo, Japan
[3] OHMOTO GUMI Co., Ltd., Okayama, Japan
[4] Preferred Robotics, Inc., Tokyo, Japan
2247024@stu.nit.ac.jp, k-ishika@nit.ac.jp

Abstract –

The pneumatic caisson method, which is used in the construction of bridge piers and other structures, is used in a variety of different sites. Currently, many processes in the pneumatic caisson method in Japan are carried out remotely. However, In Japan, the declining birthrate and aging population have created a shortage of experienced field workers. Therefore, research into the automation of the pneumatic caisson method is being actively conducted in Japan.

In this paper, we describe the results of experiments using an actual machine to test a method using the greedy algorithm with the purpose of automating the pneumatic caisson method. Our research group has previously proposed a method using the greedy algorithm for optimizing the excavation process. In this paper, we have reviewed the cost calculation equation and conducted experiments in a test field using an actual excavator. As a result of these experiments, we were able to achieve a construction speed equivalent to actual construction.

Keywords –

Automatic construction; The pneumatic caisson method; Actual machine test; Job scheduling; Process optimization; Greedy algorithm

1 Introduction

The pneumatic caisson method, which is a construction method for burying structures such as bridge piers and underground pumping plants, is used in a variety of different sites. In the pneumatic caisson method, as shown in Figure 1, a workspace is provided at the bottom of the concrete caisson. Rails are installed in the ceiling of the workspace, and an excavator is suspended from the rails. The excavator moves by traveling on and turning around these rails. By removing the soil at the bottom of the caisson using this excavator, the caisson sinks underground by its own weight and is buried. The excavated soil is loaded into an earth bucket and carried out aboveground through a material shaft. In the pneumatic caisson method, compressed air is blown into the workspace at the same pressure as the water pressure to prevent groundwater from entering the workspace. As a result, the pressure in the workspace increases as the caisson sinks. Construction work under high pressure increases the physical burden on field workers.

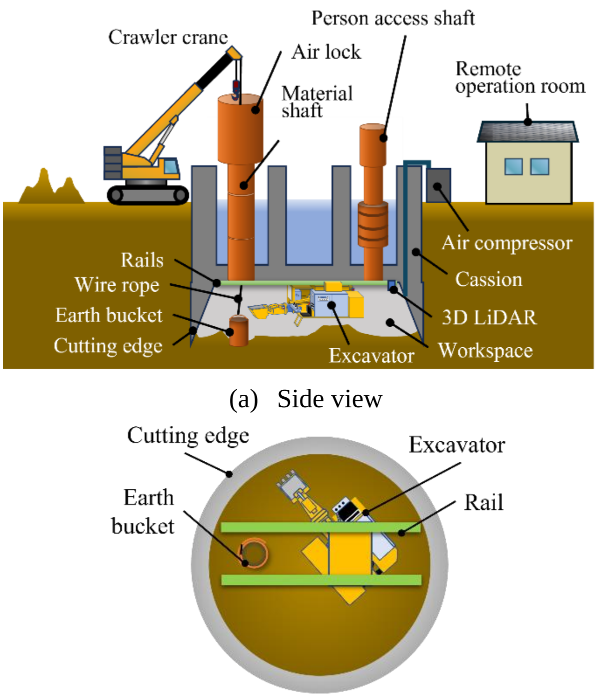

(a) Side view

(b) Diagram of workspace from above

Figure 1. Pneumatic caisson method overview

For this reason, many of the processes involved in the pneumatic caisson method in Japan are carried out remotely. However, In Japan, the declining birthrate and aging population have created a shortage of experienced field workers. For this reason, research into the automation of the pneumatic caisson method is being actively carried out in Japan.

In our previous research, we defined the excavation field and temporary soil storage area and developed a system that loads soil into an automatically recognized earth bucket or disposes of soil at the temporary soil storage area by excavating the soil at the excavation positions within the field. We have confirmed the effectiveness of this system through experiments at construction sites [1, 2, 3, 4]. Also, with the purpose of achieving automatic excavation of the entire workspace, excluding excavation under the cutting edge, we proposed a method of optimizing the excavation position and soil disposal position given to the Automatic Excavation System using the linear programming method, and compared the results with actual construction in a simulation experiment. The results showed that the proposed method achieved good results, with a volume of soil of 28.5 m^3 taking 74 minutes, compared to 98 minutes in actual construction [5].

In this paper, we describe the results of experiments in a test field using a method for optimizing excavation positions and soil disposal positions for an Automatic Excavation System, which was developed for automatic excavation of the entire workspace, excluding excavation under the cutting edge.

2 Relational Works

In Japan, there has been a lot of research into construction automation due to the shortage of manpower in the construction and civil engineering industries caused by the declining birthrate and aging population. Much of this research has focused on automating general construction machinery used in outdoor environments such as dam construction [6, 7, 8, 9, 10]. Research related to excavation planning includes the work of TERENZI et al. [11, 12, 13]. TERENZI et al. propose a method for automating back shovel excavators that divides the wide-area excavation plan into a global plan and a local plan. The global plan is treated as a Coverage Problem, and the order of the cells is determined using graph navigation algorithms. There is also research on autonomous mobile robot behavior planning, such as the research of LI et al. [14, 15].

There has also been a lot of research into the automation of the pneumatic caisson method [16, 17, 18]. In particular, in the research by TAKADA et al. [18], a job scheduling algorithm for multiple excavators is proposed using the Munkres algorithm based on the positional relationship between the soil mountain and the excavator bucket. This method achieves cooperative work by multiple excavators using a 1/10 scale model and has achieved some results. However, the experiments using the model were conducted under optimal conditions, such as the shape of the soil mountain, and the excavation conditions did not match the actual conditions of the pneumatic caisson method. In addition, this method is one in which the location of the temporary soil storage and soil disposal is specified in advance, and the excavators are assigned to work at each location, and the definition of the temporary soil storage and soil disposal locations is done manually.

In this method, we propose a method for automatically selecting the optimal excavation positions or temporarily placing positions within the excavation field. In addition, we used an excavator that is actually used in construction for the experiment, so the experiment is in line with actual construction conditions.

3 System Configuration

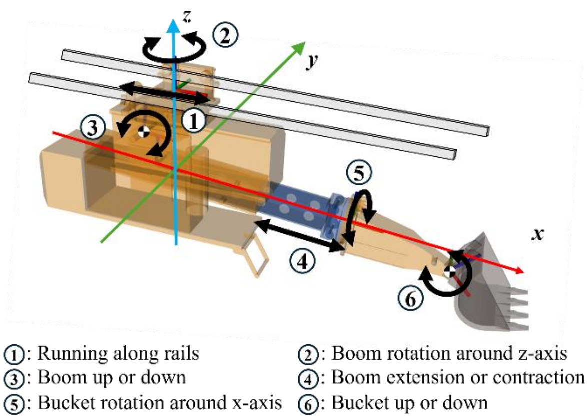

Figure 2. Diagram of excavator model

First, we will explain the excavator used in the pneumatic caisson method. Figure 2 shows a model diagram of the excavator. This excavator has six degrees of freedom: (1) running along rails, (2) boom rotation around the z-axis, (3) boom up or down, (4) boom extension or contraction, (5) bucket rotation around the x-axis and (6) bucket up or down. Basically, excavation is carried out using the (3) boom up or down, (4) boom extension or contraction and (6) bucket up or down axes, and movement is carried out using the (1) running along rails and (2) boom rotation around z-axis, and soil disposal is carried out using the (5) bucket rotation around x-axis. This excavator is operated by remote control in actual construction, so rotary encoders or potentiometers are attached to all axes. The physical quantities obtained from these are sent to the remote operation room by a wireless connection. In addition, this excavator is powered by hydraulics, as are other construction machines. The amount of stick operation on the remote-control panel in the remote operation room is sent to the excavator by wireless connection, and the hydraulic actuator is operated by opening and closing the solenoid valve. These remote-control functions are used to automate the excavator. In addition, the excavation method of the excavator is different from that of the back shovel excavator, and it excavates by scooping up the soil from below.

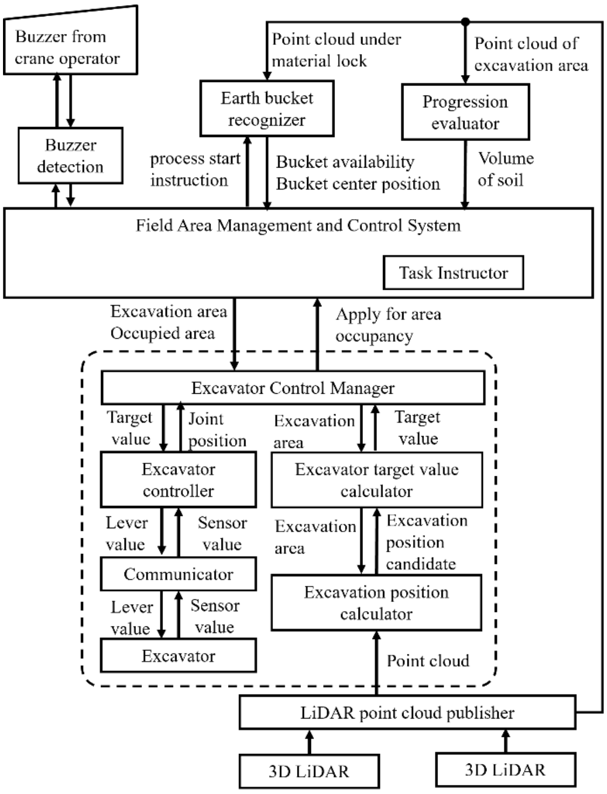

Figure 3. Diagram of the automatic excavation system configuration

Figure 3 shows an overview of the system. This system is based on the Automatic Excavation System [1] that we have been developing. It is composed of a group of software that mainly consists of the Field Area Management and Control System that manages the entire field, and a group of software that mainly consists of the Excavator Control Manager that manages the excavator. This system is a new addition to the former Field Area Management and Control System, adding a Task Instructor to instruct excavators on their tasks and where to move to. The Task Instructor instructs excavators on their tasks and where to move to, based on the volume of soil in the excavation area, the condition of the excavator and the earth bucket.

The process is as follows: First, the Excavator Control Manager requests the Task Instructor to perform a task. The Task instructor, having received the request, instructs the excavator on the work to be done, the excavation positions or the destination of the soil disposal, according to the volume of soil in the excavation area and the state of the earth bucket. Next, the Excavator Control Manager requests the Field Area Management and Control System to provide a route to the destination received from the Task Instructor. The Field Area Management and Control System then returns to the Excavator Control Manager the shortest route to the destination without coming into contact with any obstacles.

4 Methodology

In the normal excavation process of the pneumatic caisson method, excavation begins in the center of the workspace, leaving the soil near the inner wall, called the cutting edge, in place. After that, the sinking of the caisson begins by removing the soil under the cutting edge. The purpose of this research is to achieve automatic excavation of the entire central area of the workspace, excluding excavation under the cutting edge. Our research group proposed a method of optimization by replacing the excavation process of the pneumatic caisson method with a transport problem of soil [5]. The following constraints are set in this replacement:

1. Constraints on the excavator
   - The excavator can move only on rails.
   - The excavator moves by traveling and turning on the rails, at which time the speed of movement is assumed to be constant.
   - The time required for one excavation and disposal of the soil is assumed to be constant.
   - Not to excavate under the caisson cutting edge or to fill up the soil around the cutting edge.
   - The volume of soil that can be moved in one excavation depends on the size of the excavator bucket, and the excavator that our research group is targeting is 0.25 m^3.
   - When there are multiple excavators on the same rail, each one has a limited range of movement.
2. Constraints on the Earth Bucket
   - While there is no earth bucket in the workspace, soil cannot be carried out of the caisson.
   - The capacity of the earth bucket is constant at 1 m^3.
   - Only one excavator can load soil into one earth bucket at a time.
   - The time required for a full earth bucket to rise and be returned to the workspace again is

assumed to be constant. The time required depends on the length of the material shaft. Furthermore, the length depends on the amount of sinking of the caisson, but the amount of sinking is only a few tens of centimeters per day. Therefore, note that the time required does not change over one day.

- The number of earth buckets that can be loaded at one time is limited to the number of material shafts.
- The location of the earth bucket is limited to directly below the material shaft.

3. Constraints on the excavation field
   - Excavation cells are cells that divide the excavation field into grid-like sections, and the size of each cell is 0.5 x 0.5 m. Here, the cell size is set to 0.5 m to ensure that there is no excavation left when excavating adjacent cells, as the excavator bucket width is 880 mm.
   - The goal of excavation is to excavate all cells to the target depth.

We defined an objective function like Equation 1 for the above constraints. Here, N is the number of times the earth bucket is raised during construction, T_B is the time when the earth bucket is not in the workspace, T_{Ei} is the time taken for excavation and disposal of soil, T_{movei} is the time taken to move to the excavation and disposal location, and the subscript i indicates one operation.

$$\text{Minimize } T = \sum_{i=1}^{I} \left(T_{E_i} + T_{move_i} \right) + T_B N \tag{1}$$

The objective function was solved using the greedy algorithm. The greedy algorithm is one of the methods used to solve optimization problems. The greedy algorithm obtains the optimal solution by dividing the elements of the problem into subproblems, evaluating each of them independently, and incorporating them in order of their evaluation values. For example, the greedy algorithm is used in the scheduling problem of trucks and yard cranes at quay [19, 20]. The reason we chose the greedy algorithm in this method is that it is easier to implement than other algorithms and has a fast computational time.

In previous research, we have proposed a method of dividing the excavation field into a grid, calculating the movement cost of each cell with coordinates (i, j) using Equation 2, and selecting the cell with the lowest cost, and have evaluated this method through simulation [5].

$$cost_{(i,j)} = L_{(i,j)} - (G_{(i,j)}/R) \tag{2}$$

Here, $L_{(i,j)}$ is the distance from the excavation cell with coordinates (i, j) to the earth bucket, $G_{(i,j)}$ is the volume of soil in the excavation cell with coordinates (i, j), and R is the available capacity of the earth bucket.

However, when the cost calculation formula in Equation 2 was implemented in an actual machine and experiments were conducted, when the available capacity of the earth bucket became low, the excavator would select an excavation cell that was far away from the earth bucket and had a large volume of soil, and it did not operate efficiently.

In this paper, we will revise this movement cost calculation formula and propose a method that uses Equation 3 for excavation and Equation 4 for soil disposal. Here, $L_{mt(i,j)}$ is the Euclidean distance from the excavation cell at coordinates (i, j) to the material shaft, $V_{(i,j)}$ is the volume of soil in the excavation cell at coordinates (i, j), and $D_{(i,j)}$ is the minimum Euclidean distance from coordinates (i, j) is the minimum value of the Euclidean distance from the coordinate (i, j) to the cell where the soil is temporarily placed, and $L_{rovo(i,j)}$ is the Euclidean distance from the excavation cell at coordinates (i, j) to the excavator's cutting edge, and α, β, γ and δ are weighting coefficients. In addition, $L_{mt(i,j)}$, $V_{(i,j)}$, $D_{(i,j)}$, and $L_{rovo(i,j)}$ are normalized by their respective maximum values. Also, u is a coefficient that changes depending on whether or not an earth bucket is present and is when there is one and when there is not. The earth bucket shape is recognized from the point cloud data measured by the 3D LiDAR attached to the ceiling. When recognized, the position of the opening at the top of the earth bucket and the volume of soil loaded are obtained. The recognition program is not described in detail in this paper, but it is a high-speed version of the automatic recognition program developed by OSAKI et al. [2].

The following actions are selected based on whether or not an earth bucket is present, as determined by the recognition program:

1. When an earth bucket is placed under the material shaft.

   When excavating, the cell with the lowest cost is selected using the calculation in Equation 3. When disposing of soil, the position of the recognized earth bucket is returned.

2. When the earth bucket is not placed under the material shaft.

   When excavating, the cell with the lowest cost calculated using Equation 3 is selected. When disposing of soil, the cell with the lowest cost calculated using Equation 4 is selected. If the soil mountain is allowed to continue being temporarily placed in the same cell, it will become too high and interfere with the movement of the excavator. Therefore, if the distance from the highest point of the soil mountain to the ceiling becomes 1.9 m or less, the soil is disposed of in the excavation cell with the lower movement cost. This value was determined with a margin of safety, as the bottom of the excavator is 1.6 m from the ceiling.

$$cost_{e(i,j)} = \alpha_e L_{mt(i,j)}{}^u + \beta_e V_{(i,j)}{}^{-1} + \gamma_e D_{(i,j)}{}^u + \delta_e L_{rovo(i,j)} \quad (3)$$

$$cost_{d(i,j)} = \alpha_d L_{mt(i,j)} + \beta_d V_{(i,j)} + \gamma_d D_{(i,j)} + \delta_d L_{rovo(i,j)}{}^{-1} \quad (4)$$

5 Evaluation Experiment

5.1 Experiment Overview

To evaluate this method, we conducted an evaluation test using an actual machine in a test field. Figure 4 shows the excavation field and the location of the material shaft. The excavation field is a 3 x 3 m square centered on (x, y) = (0.0 m, –1.0 m), and the target excavation depth is 0.5 m from the ground surface. The size of the excavation field was determined based on the maximum size of our test field. The size is small, but in actual construction sites where we have conducted experiments, the size has been the same or smaller than this. In this experiment, we measured the time required to excavate all the cells in the excavation field to the target depth.

The material shaft is a circle with a radius of 1.5 m centered on (x, y) = (0.0 m, 3.0 m), and the soil disposal bucket is placed within this circle. The earth bucket is placed and carried out directly below the material shaft by crane. The time from when a full earth bucket is carried out of the workspace to when it is placed in the workspace again is about 4 minutes. This is the same as in actual construction. The earth bucket can load 1 m^3 of soil at a time. In this experiment, the total volume of soil excavated is calculated based on the number of full earth buckets.

In addition, the weighting coefficients for Equation 3 are α = 0.2, β = 0.3, γ = 0.3, δ = 0.2, and the weighting coefficients for Equation 4 are α = 0.2, β = 0.0, γ = 0.5, δ = 0.3. These weighting coefficients were determined by repeated experiments.

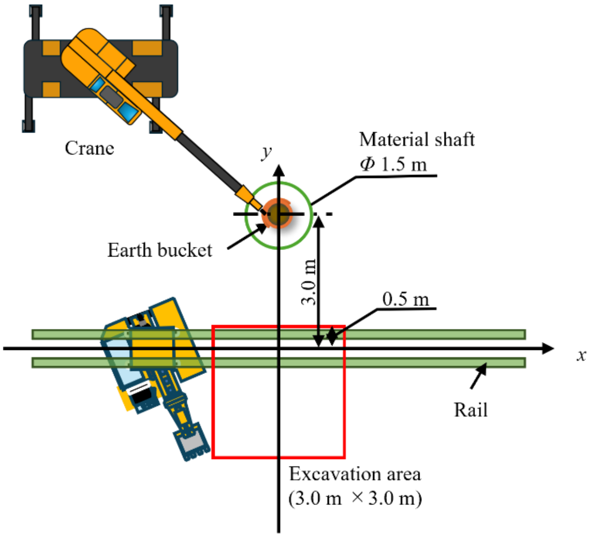

Figure 4. Diagram of Evaluation Experiment

5.2 Results and Discussion

The experiment is shown in Figures 5 and 6. The right side of both figures shows the test field. The left side of both figures shows the display screen of the Automatic Excavation System. The red frame shows the excavation field, and the green frame shows the excavation cells selected by the method. The Automatic Excavation System controls the excavator so that the blade tip is at the center of the green frame, and then performs excavation or soil disposal at that point. The heat map in both figures shows the height of the ground, with red indicating low areas and purple indicating high areas.

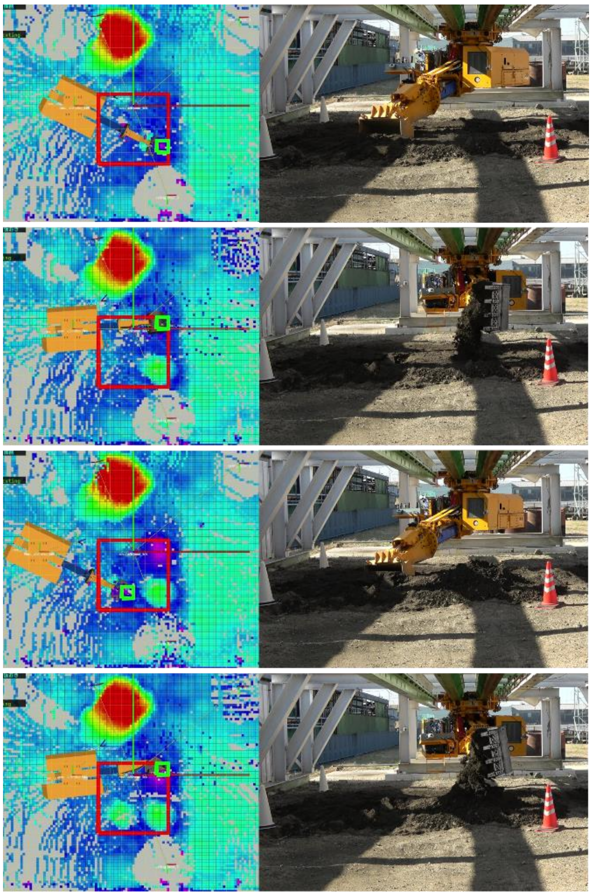

Figure 5. Experimental result when the earth bucket is not placed under the material shaft

Figure 5 shows the situation when the earth bucket is not placed under the material shaft. In the top row, the excavator is digging the cell with the lowest cost calculated using Equation 3. In the second row from the top, the excavator is temporarily placing the earth in the cell with the lowest cost calculated using Equation 4. The two bottom rows are the same as the top row, but the cell that was excavated the first time is no longer selected due to a decrease in the volume of soil. This process is repeated until the earth bucket is placed under the material shaft. Looking at the entire process, the earth in the excavation field is moved towards the material shaft. When disposing of soil in temporary soil storage, cells with high soil mountains were passed over in the calculations, and cells with low costs were selected next. As a result, the distance from the highest point of the soil mountain to the ceiling was never less than 1.6 m, and there were no problems with the movement of the excavator.

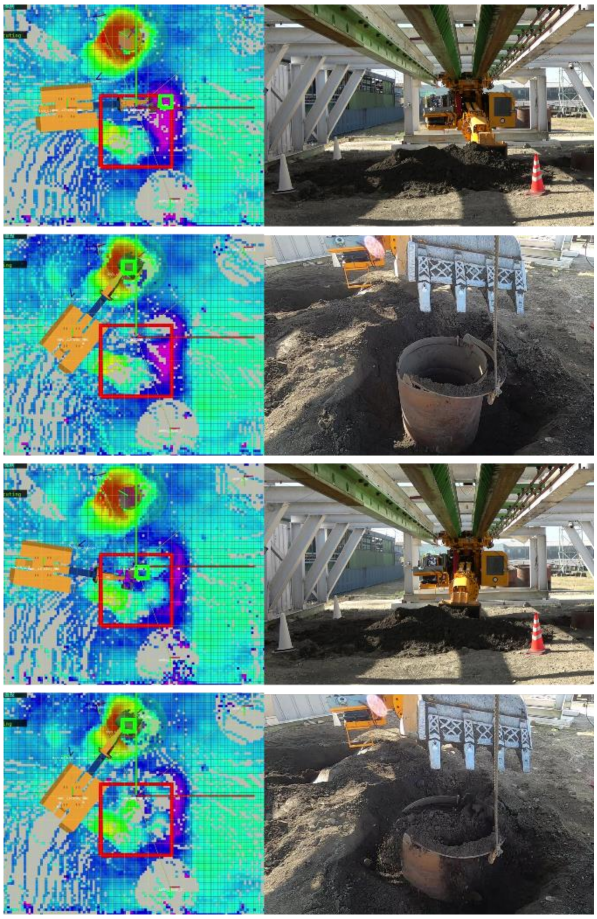

Figure 6. Experimental result when the earth bucket is placed under the material shaft

Figure 6 shows the situation when the earth bucket is placed under the material shaft. The earth is loaded until the Automatic Excavation System judges that the bucket is full. The top row in Figure 6 shows the state after the earth bucket is placed under the material shaft. The excavation cell with the lowest cost, as calculated by Equation 3, is excavated. The second row from the top shows the situation where the earth is loaded into the earth bucket. The location where the earth is directly thrown is the location of the recognized earth bucket, which also matches the actual location where it is placed. In addition, the recognition rate for the earth bucket was 100% out of the 30 times it was loaded during the evaluation experiment. The accuracy of the recognition posture was an error of 0.07 m in position and 5.73 degrees in orientation.

Table 1. Required time for each state of the excavator

Step	Case	Time [h:min:s]	Excavated soil volume [m^3]
1~6	Temporary	0:06:22	—
7~11	Disposal	0:06:27	1.00
12~16	Temporary	0:05:20	—
17~22	Disposal	0:09:42	1.00
23~27	Temporary	0:04:42	—
28~35	Disposal	0:08:49	1.00
36~40	Temporary	0:05:22	—
41~45	Disposal	0:08:19	1.00
46~49	Temporary	0:04:47	—
50~56	Disposal	0:10:20	1.00
Total		1:10:00	5.00
Actual construction process time		1:07:06	5.00

Table 1 shows the results of measuring the time required for each operation of the excavator. In this table, the process from when the excavator excavates the soil and moves it to when it is temporarily placed or directly thrown is considered to be one step. As a result, it took 56 steps and 1 hour and 10 minutes. During actual construction, the same conditions were completed in 1 hour, 7 minutes, and 6 seconds, so it can be said that effective results were obtained.

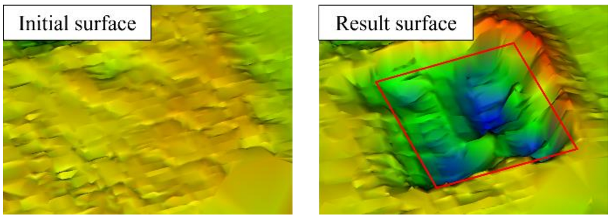

Figure 7. Ground surface before and after the experiment

Figure 7 shows the changes in the ground before and after excavation, with the left side showing the state before the experiment began and the right side showing the state at the end of the experiment. The excavator is located on the left side of both figures, and the material shaft is located on the upper side. The colors of the ground in the figures indicate the height of the ground, with blue indicating low ground and red indicating high ground. The red frame in the figure on the right shows the excavation field. Looking at the excavation field in the ground in the figure on the right, you can see that the left side of the excavation field is higher than the right side. Also, looking at the area outside the excavation field in the figure, you can see that the left side has been excavated and the right side has been piled up with soil. The standard deviation of the depth to the ground surface after excavation is 0.27 m with respect to the target depth.

Because the excavation operation of this system measures the ground height using 3D LiDAR, the bucket cutting edge is placed at that point, and excavation is carried out to the target depth from there. However, the excavation positions are not the center of the excavation cells, but the starting points of excavation in front of the excavation cells as seen from the excavator. Therefore, when the excavator excavates a cell that is further away from the excavator than the cell that has already been excavated, it is thought that the excavator will excavate deeper than the excavation cell. From this, there is still room for improvement in the excavation method of this system.

6 Conclusion and Future Works

In this paper, we propose a method using the greedy algorithm for the purpose of automating the pneumatic caisson method, and we confirmed that we achieved a construction speed equivalent to actual construction in experiments using an actual machine.

In the future, we plan to review weighting coefficients and cost calculation equations, and consider other optimization algorithms, with the purpose of minimizing the required time. In addition, in the large-scale pneumatic caisson method, multiple excavators are used. Our research group has achieved the automatic excavation and soil disposal of multiple excavators without causing them to collide with each other. Therefore, we plan to propose a method for multiple excavators.

References

[1] K. Ishikawa, H. Harada, H. Osaki, S. Tsugawa, S. Tachibana, H. Fujisawa, T. Terui, K. Nakamura and Y. Inagawa. Automatic Excavation System with Multiple Excavators in the Pneumatic Caisson Method. *Journal of Robotics and Mechatronics*, 36(4):961–972, 2024.

[2] H. Osaki, K. Ishikawa, Y. Inagawa, T. Terui, S. Tachibana and S. Tsugawa. Development of Automatic Excavation System for Pneumatic caisson method -Overhead Traveling Excavator Automation and Earthen Bucket Recognition-. In *Proceedings of the Symposium on Construction Execution and Construction Machinery*, pages 159–164, Tokyo, Japan, 2022. In Japanese.

[3] OBAYASHI CORPORATION. Demonstration of the automated excavation system for the pneumatic caisson method at the construction site of the Hanshin Namba Line in Osaka, Japan. On-line:

https://www.obayashi.co.jp/news/detail/news20230616_2.html, Accessed: 12/01/2024. In Japanese.

[4] Y. Betsui, Y. Inagawa, T. Terui, K. Nakamura, T. Ogata, H. Fujisawa, S. Tachibana, and S. Tsugawa. A Study on Overhead Travelling Excavator Automation -An Excavator Simulator Development and Bucket Trajectory Control-. In *SICE SI 2021*, pages 2088–2089, Online, Japan, 2021.

[5] H. Harada, K. Ishikawa, T. Terui, Y. Inagawa, S. Tachibana and S Tsugawa. Optimization of Excavation Process in the Pneumatic Caisson Method. In *SICE Festival 2024 with Annual conference*, pages 514–517, Kochi, Japan, 2024.

[6] L. Zhang, J. Zhao, P. Long, L. Wang, L. Qian, F. Lu, X. Song and D. Manocha. An autonomous excavator system for material loading tasks. *Science Robotics*, 6(55):eabc3164, 2021.

[7] E. Halbach, A. Kolu and R. Ghabcheloo. Automated Pile Transfer Work Cycles with a Robotic Wheel Loader. In *17th International Conference on Computing in Civil and Building Engineering*, Tampere, Finland, 2018.

[8] Y. Yang, L. Zhang, X. Cheng, J. Pan and R. Yang. Compact Reachability Map for Excavator Motion Planning. In *2019 IEEE/RSJ International Conference on Intelligent Robots and Systems (IROS)*, pages 2308–2313, Macau, China, 2019.

[9] H. Murayama, T. Kawabe, M. Inagawa, K. Yoshizawa, M. Ishibashi, T. Takei and K. Nagatani. Demonstration of Snow Removal Work by Wheel Loader in an Environment Surrounded by Obstacles. *Journal of Robotics and Mechatronics*, 35(5):1251–1266, 2023.

[10] H. Yoshida, T. Yoshimoto, D. Umino and N. Mori. Practical Full Automation of Excavation and Loading for Hydraulic Excavators in Indoor Environments. In *2021 IEEE 17th International Conference on Automation Science and Engineering (CASE)*, pages 2153–2160, Lyon, France, 2021.

[11] L. Terenzi and M. Hutter. Towards autonomous excavation planning. *IEEE Transactions on Field Robotics*, 1(1):292–317, 2024.

[12] J. Seo, S. Lee, J. Kim and S. Kim. Task planner design for an automated excavation system. *Automation in Construction*, 20(7):954–966, 2011.

[13] S. Park, J. Kim, K. Cho and J. Seo. Integrating Task Component Design in Excavator–Truck Operation Planning: Enhancing Automation Systems through a Web-Based System. *Applied Sciences*, 14(14):6052, 2024.

[14] W. Li, H. Li, Y. Wang, and Y. Han. Optimizing flexible job shop scheduling with automated guided vehicles using a multi-strategy-driven genetic algorithm. *Egyptian Informatics Journal*, 25(1):100437, 2024.

[15] B. Xin, S. Lu, Q. Wang, F. Deng, X. Shi, J. Cheng and Y. Kang. Simultaneous scheduling of processing machines and automated guided vehicles via a multi-view modeling-based hybrid algorithm. *IEEE Transactions on Automation Science and Engineering*, 21(3):4753–4767, 2023.

[16] N. Negishi, A. Iwasaki and T. Kataoka. Development of a construction management system for the pneumatic caisson method -Construction management aids and caisson excavator automation-. In *Proceedings of the Symposium on Construction Execution and Construction Machinery*, pages 126–129, Tokyo, Japan, 2023. In Japanese.

[17] N. Negishi, T. Tsuneki, K. Kikuchi, T. Kondo, T. Koyo, A. Kamei and K. Hayakawa. A Study on Autonomous Operation System of Caisson Shovels in High Air Pressure and Narrow Underground Space (Demonstration of Trajectory Tracking Control). In *The 4th International Conference on Design Engineering and Science: ICDES2017*, Aachen, Germany, 2017.

[18] K. Takada, R. Sato, S. Sato, M. Ito, R. Tsuchiya, K. Kikuchi, M. Shindo, A. Kamei and T. Kondo. Autonomous Operation System of Caisson Shovels in Narrow Underground Space at High Air Pressure (Development of a Job Scheduling Algorithm using a 1/10 Caisson Platform). *Journal of Japan Society for Design Engineering*, 57(8):381–396,2022.

[19] K. Li and L. Tang. A Tabu Search Algorithm for the Integrated Truck Scheduling and Storage Allocation in Quay. In *2009 Second International Symposium on Computational Intelligence and Design*, pages 275–278, Changsha, China, 2009.

[20] L. Kong, M Ji, and Z Gao. Joint optimization of container slot planning and truck scheduling for tandem quay cranes. *European Journal of Operational Research*, 293(1):149–166, 2021.